Environmental Science & Technology

pubs.acs.org/est

Article

Reactivity of Chlorine Radicals ($Cl^{\bullet}$ and $Cl_2^{\bullet-}$) with Dissolved Organic Matter and the Formation of Chlorinated Byproducts

Yu Lei, Xin Lei, Paul Westerhoff, Xinran Zhang, and Xin Yang*

Cite This: *Environ. Sci. Technol.* 2021, 55, 689–699

Read Online

ACCESS | Metrics & More | Article Recommendations | Supporting Information

ABSTRACT: Chlorine radicals, including $Cl^{\bullet}$ and $Cl_2^{\bullet-}$, can be produced in sunlight waters (rivers, oceans, and lakes) or water treatment processes (e.g., electrochemical and advanced oxidation processes). Dissolved organic matter (DOM) is a major reactant with, or a scavenger of, $Cl^{\bullet}$ and $Cl_2^{\bullet-}$ in water, but limited quantitative information exists regarding the influence of DOM structure on its reactivity with $Cl^{\bullet}$ and $Cl_2^{\bullet-}$. This study aimed at quantifying the reaction rates and the formation of chlorinated organic byproducts produced from $Cl^{\bullet}$ and $Cl_2^{\bullet-}$ reactions with DOM. Laser flash photolysis experiments were conducted to quantify the second-order reaction rate constants of 19 DOM isolates with $Cl^{\bullet}$ ($k_{DOM-Cl\bullet}$) and $Cl_2^{\bullet-}$ ($k_{DOM-Cl2\bullet-}$), and compare those with the hydroxyl radical rate constants ($k_{DOM-\bullet OH}$). The values for $k_{DOM-Cl\bullet}$ ($(3.71 \pm 0.34) \times 10^8$ to $(1.52 \pm 1.56) \times 10^9$ M_C^{-1} s^{-1}) were orders of magnitude greater than the $k_{DOM-Cl2\bullet-}$ values ($(4.60 \pm 0.90) \times 10^6$ to $(3.57 \pm 0.53) \times 10^7$ M_C^{-1} s^{-1}). $k_{DOM-Cl\bullet}$ negatively correlated with the weight-averaged molecular weight (M_W) due to the diffusion-controlled reactions. DOM with high aromaticity and total antioxidant capacity tended to react faster with $Cl_2^{\bullet-}$. During the same experiments, we also monitored the formation of chlorinated byproducts through the evolution of total organic chlorine (TOCl) as a function of chlorine radical oxidant exposure (CT value). Maximum TOCl occurred at a CT of $4-8 \times 10^{-12}$ M·s for $Cl^{\bullet}$ and $1.1-2.2 \times 10^{-10}$ M·s for $Cl_2^{\bullet-}$. These results signify the importance of DOM in scavenging chlorine radicals and the potential risks of producing chlorinated byproducts of unknown toxicity.

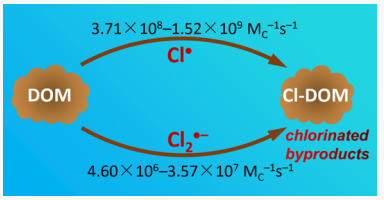

KEYWORDS: *chlorine radicals, dissolved organic matter, reaction rate constants, chlorinated byproducts*

INTRODUCTION

Chlorine atoms ($Cl^{\bullet}$) and dichlorine radical anions ($Cl_2^{\bullet-}$) impact photochemical processes in radical-mediated advanced oxidation processes (AOPs) for water and wastewater treatment and in natural waters.[1−3] $Cl^{\bullet}$ and $Cl_2^{\bullet-}$ can be generated from the reactions of sulfate radicals with chloride ions (Cl^-), the electrochemical treatment of high salinity wastewater, or the photolysis of free chlorine.[4,5] $Cl^{\bullet}$ (E^0 = 2.55 V vs SHE) and $Cl_2^{\bullet-}$ (E^0 = 2.13 V vs SHE) are highly reactive in transforming a variety group of organic micropollutants.[4,6,7] Our research group has determined the reactivity of dozens of trace organic contaminants (TrOCs) toward $Cl^{\bullet}$ (k = $(3.10 \pm 0.50) \times 10^9$ to $(4.08 \pm 0.24) \times 10^{10}$ M^{-1} s^{-1}) and $Cl_2^{\bullet-}$ (k = < 1×10^6 to $(2.78 \pm 0.16) \times 10^9$ M^{-1} s^{-1}).[8] The transformation rates of TrOCs are greatly reduced in the presence of dissolved organic matter (DOM), which is ubiquitous in water and wastewater and significantly scavenges radicals.[6,9−11] However, few studies have reported the reaction rates between $Cl^{\bullet}$ or $Cl_2^{\bullet-}$ and DOM,[12] especially DOM from different sources.

The only reaction rate constant reported was 1.56×10^8 M_C^{-1} s^{-1} for $Cl^{\bullet}$ reacting with Suwannee River NOM, which was estimated from a modeling analysis of several radicals' steady-state concentrations in the UV/chlorine treatment.[13] The reaction rate constants of $Cl_2^{\bullet-}$ with DOM (k = 10∼1000 L mg_C^{-1} s^{-1}) were assumed based on the reactivity of $Cl_2^{\bullet-}$ toward organic compounds.[14] DOM in water from different regions has various components with various function groups, and they inevitably exhibit different reactivities toward oxidants, as indicated by studies reporting DOM reactivity with $^{\bullet}OH$, $SO_4^{\bullet-}$, or $CO_3^{\bullet-}$.[9,15,16] The $^{\bullet}OH$ rate constants with DOMs ranged from $(1.4 \pm 0.2) \times 10^8$ to $(4.5 \pm 0.5) \times 10^8$ M_C^{-1} s^{-1}, and the rate constants of $^{\bullet}OH$ with bulk effluent organic matter (EfOM) could exceed $\sim 10^9$ M_C^{-1} s^{-1}.[9,10,17,18] DOM also exhibited diverse reactivity toward $SO_4^{\bullet-}$ ($(1.84 \pm 0.07) \times 10^7$ to $(2.48 \pm 0.12) \times 10^8$ M_C^{-1} s^{-1}) and $CO_3^{\bullet-}$ ($(1.8 \pm 0.5) \times 10^5$ to $(3.4 \pm 1.1) \times 10^6$ M_C^{-1} s^{-1}), depending on DOM properties.[15,16,19−21] Meanwhile, the rate constants of DOM with $^{\bullet}OH$ and $CO_3^{\bullet-}$ have been reported to correlate with the DOM properties, including specific UV absorbance at 254 nm ($SUVA_{254}$), fluorescence index (FI), and weight-averaged molecular weight (M_W).[15,22,23] Establishing relationships between the reactivity of DOM with radicals and the physicochemical properties of DOM is helpful in understanding the reaction mechanisms and can be used to predict the reactivity of diverse DOM.[10,22] Developing the relation-

Received: August 19, 2020
Revised: December 9, 2020
Accepted: December 9, 2020
Published: December 21, 2020

https://dx.doi.org/10.1021/acs.est.0c05596
Environ. Sci. Technol. 2021, 55, 689–699

Table 1. DOM Properties and the Second-Order Rate Constants for the Reactions of $Cl^{\bullet}$, $Cl_2^{\bullet-}$, and $^{\bullet}OH$ with DOM

No.	full name	abbreviation	M_W[a] (Da)	E2/E3[b]	FI[c]	$SUVA_{254}$[d] ($L\ mg^{-1}\ m^{-1}$)	TAC[e] (mgGA/mg_C)	$k_{DOM-Cl^{\bullet}}$ ($10^8\ M_C^{-1}\ s^{-1}$)	$k_{DOM-Cl_2^{\bullet-}}$ ($10^7\ M_C^{-1}\ s^{-1}$)	$k_{DOM-^{\bullet}OH}$ ($10^8\ M_C^{-1}\ s^{-1}$)
1	Suwannee River I NOM[f,g]	SRNOM I	2200	4.45	1.35	4.36	0.26	3.71 ± 0.34	1.71 ± 0.21	3.0[13]
2	Suwannee River II NOM[h]	SRNOM II	1940[o]	4.85	1.39	4.00	0.24	4.12 ± 0.32	1.64 ± 0.35	
3	Nordic Lake NOM	NLNOM	1795[o]	4.60	1.44	4.03	0.28	4.50 ± 0.30	1.31 ± 0.17	
4	Upper Mississippi River NOM	UMNOM	1510	4.67	1.78	3.55	0.15	5.93 ± 0.29	2.18 ± 0.18	
5	Suwannee River II FA[i]	SRFA	2019	4.61	1.34	4.13	0.30	6.60 ± 0.63	2.27 ± 0.21	1.60 ± 0.24[9] 2.06 ± 0.09[18]
6	Pahokee Peat FA	PPFA	1894	4.17	1.27	6.25	0.19	10.17 ± 0.80	2.75 ± 0.53	
7	Nordic Lake FA	NLFA	1698[o]	4.28	1.41	4.64	0.34	10.38 ± 1.02	2.93 ± 0.36	
8	Pony Lake FA	PLFA	1517	5.00	1.55	2.52	0.29	7.40 ± 0.78	0.99 ± 0.10	6.9 ± 0.53[18]
9	Pahokee Peat HA[j]	PPHA	2977	2.81	0.89	6.90	0.31	4.26 ± 0.42	2.61 ± 0.48	
10	Leonardite HA	LHA	3320[o]	2.54	1.24	6.91	0.39	5.20 ± 0.27	3.57 ± 0.53	
11	Elliott Soil IV HA	ESHA	3089	2.33	0.84	6.51	0.21	5.30 ± 0.49	2.80 ± 0.61	1.21 ± 0.09[18]
12	Salt River HPOA[k]	SR−HPOA	1584	4.84	1.33	2.75	0.13	9.85 ± 0.45	0.61 ± 0.11	
13	Salt River HPON[l]	SR−HPON	1023	5.49	1.21	1.88	0.07	11.20 ± 0.64	0.75 ± 0.13	
14	Salt River TPIA[m]	SR−TPIA	980[o]	6.31	1.46	2.13	0.11	12.60 ± 1.15	0.82 ± 0.12	
15	Salt River TPIN[n]	SR−TPIN	892[o]	6.82	1.62	2.01	0.09	15.17 ± 1.56	0.98 ± 0.10	
16	Saguaro Lake HPOA	SL−HPOA	1258	9.70	1.89	2.42	0.06	5.64 ± 0.33	0.46 ± 0.09	1.73 ± 0.04[9]
17	Saguaro Lake TPIA	SL−TPIA	1104[o]	7.23	1.52	2.06	0.08	8.30 ± 0.40	0.65 ± 0.12	1.45 ± 0.02[9]
18	Nogales WWTP HPOA	WWTP HPOA	1376	5.52	1.87	1.12	0.13	8.42 ± 0.51	1.55 ± 0.29	
19	Nogales WWTP−TPIA	WWTP−TPIA	992	8.20	2.39	1.29	0.13	13.05 ± 0.89	1.37 ± 0.12	3.63 ± 0.31[9]
Averages			**1746**	**5.18**	**1.46**	**3.61**	**0.20**	**7.99 ± 0.61**	**1.68 ± 0.25**	**2.5**[17]

[a]: M_w = weight-averaged molecular weight. [b]: E2/E3 = absorbance at 254 nm divided by absorbance at 365 nm. [c]: FI = fluorescence index. [d]: $SUVA_{254}$ = specific UV absorbance at 254 nm. [e]: TAC = total antioxidant capacity, GA = gallic acid. [f]: NOM = natural organic matter. [g]: 1R101N. [h]: 2R101N [i]: FA = fulvic acid. [j]: HA = humic acid. [k]: HPOA = hydrophobic acid. [l]: HPON = hydrophobic neutral. [m]: TPIA = transphilic acid. [n]: TPIN = transphilic neutral. [o]: Estimated from the established correlation between M_W and $SUVA_{280}$ for the aquatic NOM sample.[23]

ships between the rate constants of $Cl^{\bullet}$ and $Cl_2^{\bullet-}$ with DOM of variable physicochemical properties allows future researchers to understand the variability in TrOC degradation in different sources of water.

In addition to the scavenging radicals that are capable of degrading TrOCs, concerns have also been expressed regarding the possible generation of chlorinated organic byproducts and adverse health outcomes, from the reactions of $Cl^{\bullet}$ and $Cl_2^{\bullet-}$ with DOM.[24−26] $Cl^{\bullet}$ and $Cl_2^{\bullet-}$ may react with organics via chlorine addition, single electron transfer (SET), and H-abstraction.[8,27] Among them, chlorine addition is expected as the most likely pathway leading to the formation of chlorinated byproducts.[28] In fact, the formation of chlorinated products has been observed from the reactions of $Cl^{\bullet}$ and $Cl_2^{\bullet-}$ with some organic contaminants. For example, in a $Cl_2^{\bullet-}$-dominant oxidation system (UV/persulfate with excessive Cl^-), chlorinated byproducts including O,O-dimethyl phosphorochloridothioate were observed upon the degradation of methidathion and dimethoate.[29] UV/chlorine, a process containing diverse reactive chlorine species (RCS, including $Cl^{\bullet}$ and $Cl_2^{\bullet-}$), generated more chlorinated byproducts than chlorination alone in some studies.[30−33] Studies on the dominant sources of chlorinated byproducts in AOPs remain conflicting, with some suggesting chlorinated byproducts originated mainly from the direct addition of chlorine atoms into DOM, but others inferred that the primary chlorinating agent was hypochlorous acid/hypochlorite ($HOCl/ClO^-$).[34−36] So far, there is no direct evidence to prove that $Cl^{\bullet}$ or $Cl_2^{\bullet-}$ can induce the formation of chlorinated byproducts from the reaction with DOM.

The objectives of this study are to determine the second-order rate constants of DOM with $Cl^{\bullet}$ and $Cl_2^{\bullet-}$ and their dependence with the properties of DOM, plus to quantify the $Cl^{\bullet}$ or $Cl_2^{\bullet-}$-induced formation of chlorinated byproducts. Nineteen DOM isolates from different locations were procured (Table 1), including 11 DOM isolates purchased from International Humic Substances Society (IHSS) and eight previously characterized DOM isolates fractionated from natural water and wastewater effluents in Arizona. First, the reaction rate constants with $Cl^{\bullet}$ were determined using laser flash photolysis and those with the $Cl_2^{\bullet-}$ reaction were determined using steady-state competition kinetics. Second, statistical relationships were established between the reaction rate constants and the physicochemical properties of DOM (i.e., UV/vis absorbance, fluorescence, molecular weight, total antioxidant capacity (TAC)). Third, the generation of chlorinated byproducts from the reactions of $Cl^{\bullet}$ or $Cl_2^{\bullet-}$ with DOM was quantified using total organic chloride (TOCl). The evolution profile of TOCl yield versus oxidant ($Cl^{\bullet}$ or $Cl_2^{\bullet-}$) exposure was quantified. The results of this study improve the understanding of the $Cl^{\bullet}$ and $Cl_2^{\bullet-}$ reaction kinetics and products from the reaction with DOM.

MATERIALS AND METHODS

Chemicals. Eleven DOM isolates were purchased from the International Humic Substance Society (Table 1). These include reverse-osmosis isolates from surface waters (Suwan-

https://dx.doi.org/10.1021/acs.est.0c05596
Environ. Sci. Technol. 2021, 55, 689−699

nee River, Mississippi River, and Nordic Lake), fulvic acid from surface waters (Suwannee River, Pony Lake, and Nordic Lake), and humic or fulvic acid from soils (Pahokee Peat, Leonardite, and Elliott Soil IV). A range of well-characterized hydrophobic to hydrophilic acid and neutral DOM fractions were isolated from surface waters (Saguaro Lake, Arizona; Salt River, Arizona) or wastewater effluents (Nogales wastewater treatment plant (WWTP), Arizona).[37−40] DOM from different sources (aquatic, soil, and microbial origins) and of different types (HA, FA, and EfOM) are chosen in this work because of their different structures and polarities. Previous studies by our group and Rosario-Ortiz's group showed that the DOM source and structure can result in the $^{\bullet}OH$ radical reaction rates varying by over one order of magnitude.[17,22] Our objectives are to examine the reaction kinetics and mechanisms between the $Cl^{\bullet}$ and $Cl_2^{\bullet-}$ reactions with DOM having differing sources and structures, and investigate how such differences are related to the reaction rates with $Cl^{\bullet}$ and $Cl_2^{\bullet-}$. The details of DOM fractionation experiments were depicted in Text S2. The acronyms for each DOM fraction can be identified using Table S1. Other reagents used in this study are described in Text S1. All the solutions were prepared using ultrapure water (≥18.2 MΩ).

Determination of the Reaction Rate Constants of $Cl^{\bullet}$ with DOM. The second-order reaction rate constants of DOM with $Cl^{\bullet}$ ($k_{DOM-Cl\bullet}$) were measured using a laser flash photolysis system (LKS80, Applied Photophysics). All the experiments were conducted at room temperature (25 ± 2 °C). For each sample, the kinetics signals were averaged from 10 replicate laser shots. The pH of the solutions was adjusted to 7.0 ± 0.3 by adding NaOH or $HClO_4$. The details are provided in Text S3. Briefly, $Cl^{\bullet}$ was generated by 266 nm laser photolysis of 10 mM chloroacetone (eq 1).[41]

$$CH_3COCH_2Cl + h\nu \rightarrow CH_3COCH_2^{\bullet} + Cl^{\bullet} \quad (1)$$

A conventional SCN^- competition kinetic method by fixing the SCN^- concentration was applied to determine the rate constants of $Cl^{\bullet}$ with DOM (Figure S2). The kinetics were also conducted by fixing the DOM concentration for comparison to minimize the potential interference induced by the inner filter effects of DOM. Meanwhile, a transient decay kinetics method was also applied by tracking the abatement of $Cl^{\bullet}$ absorbance for cross-validation (Figure S2). Moreover, the rate constants of $Cl^{\bullet}$ with model compounds were determined using conventional SCN^- competition kinetics.[8] The details are provided in Text S4.

Determination of Reaction Rate Constants of $Cl_2^{\bullet-}$ with DOM. A steady-state competition kinetics method using phenol as a reference compound was used to determine the reaction rate constants of $Cl_2^{\bullet-}$ with DOM ($k_{DOM-Cl2\bullet-}$). Briefly, $Cl_2^{\bullet-}$ was generated by reacting excessive Cl^- (0.5 M) with $SO_4^{\bullet-}$, which was formed upon the 254 nm UV irradiation of 5 mM $S_2O_8^{2-}$.[29] The pH of solutions was adjusted to 7.0 ± 0.3 using 4 mM phosphate buffer, and 10 mM tert-butanol (TBA) was dosed to minimize the potential effects of $^{\bullet}OH$. The competition can be analyzed using the following expression (eq 2):[15]

$$\frac{k'_{phenol([DOM=0])}}{k'_{phenol([DOM])}} = 1 + \frac{k_{DOM-Cl_2\bullet}\text{-}[DOM]}{k_{phenol-Cl_2\bullet}\text{-}[phenol]} \quad (2)$$

where [DOM] and [phenol] are the molar concentrations of DOM and phenol, respectively. The pseudo-first-order decay rate constant of phenol (k') decreased with the increase in the concentration of DOM. Given the known rate constant of $Cl_2^{\bullet-}$ with phenol ($k_{phenol-Cl2\bullet-} = (2.2 \pm 0.1) \times 10^8\ M^{-1}\ s^{-1}$ at pH 7.0),[8] the second-order rate constants of $Cl_2^{\bullet-}$ with DOM ($k_{DOM-Cl2\bullet-}$) could be obtained (Figure S3). All the errors of rate constants determined in this work were obtained at a 95% confidence interval, and triplicate tests were performed. The details are shown in Text S5.

While $ClO^{\bullet}$ is another RCS reported to form during photolysis of chlorine solutions, it was not the focus of this project. It would require different solution chemistry to selectively generate $ClO^{\bullet}$, and the $ClO^{\bullet}$ reaction kinetics would be affected by other coexisting radicals.[6,42]

DOM Characterization. The UV absorbance DOM was measured using a UV−vis spectrophotometer (UV − 2700, Shimadzu) to obtain SUVA (specific UV absorbance at 254 nm, UV_{254}/DOC) and E2/E3 (UV_{254}/UV_{365}). A fluorescence spectrometer (Aqualog, Horriba) was used to determine the FI of DOM, taken as the ratio of fluorescence at 370 nm excitation and 470/520 nm emission.[43] DOC was quantified using a total organic carbon analyzer (TOC−V_{CPH}, Shimadzu). High-performance size-exclusion chromatography (HPSEC) was used to determine the molecular weight distribution of DOM.[23] The TAC of DOM was quantified using a Folin−Ciocalteu (F−C) assay.[44] The details are presented in Text S6 and Figure S5. The physical−chemical properties of DOMs studied in this work are listed in Table 1, including the M_W, E2/E3, FI, $SUVA_{254}$, and TAC values.

TOCl and Specific Byproduct Formation. The solutions containing target DOM and precursor to generate $Cl^{\bullet}$ or $Cl_2^{\bullet-}$ were mixed and then irradiated by pulsed laser (laser duration 4∼6 ns) at pH 7.0. The photolysis of chloroacetone is not suitable for generating $Cl^{\bullet}$ for TOCl determination, as chloroacetone also contains organic chlorine. The removal of chloroacetone without interfering the TOCl analysis is not successfully achieved. Therefore, $Cl^{\bullet}$ was generated by reacting a low concentration of Cl^- (0.2 mM) with $SO_4^{\bullet-}$, and a careful evaluation was conducted (Text S7).[45,46] $Cl_2^{\bullet-}$ was generated by reacting excessive Cl^- (0.5 M) with $SO_4^{\bullet-}$. To achieve different $Cl^{\bullet}$ or $Cl_2^{\bullet-}$ exposure, the samples were treated under multiple pulses of laser irradiation, rotating and moving the samples between each laser irradiation to make the reactor receive nearly equal irradiation (Scheme S1). After irradiation, the samples were either extracted using activated carbon for TOCl determination or subjected to the volatile trichloromethane (TCM) analysis. The concentrations of TOCl were determined on a TOX analyzer (Xplorer, TE Instruments, the Netherlands), and the details are described in Text S7. The concentrations of TCM were determined according to the USEPA Method 551.1. The samples were extracted using methyl *tert*-butyl ether (MTBE) and analyzed using a gas chromatograph (Agilent 7890A) system equipped with an electron capture detector and a HP-5 fused silica capillary column (30 m × 0.25 mm, 0.25 mm, Agilent J&W Scientific).[47] The detection limit of TCM is 0.1 μg L^{-1}. The reactive chlorine oxidant ($Cl^{\bullet}$ or $Cl_2^{\bullet-}$) exposure (units of M·s) was calculated from the integral area of the optical absorption traces of $Cl^{\bullet}$ or $Cl_2^{\bullet-}$ (Figure S6).

RESULTS AND DISCUSSION

Rate Constants between DOM and $Cl^{\bullet}$. Table 1 summarizes the obtained rate constants from the laser flash photolysis experiments, the raw data and data analysis results

https://dx.doi.org/10.1021/acs.est.0c05596
Environ. Sci. Technol. 2021, 55, 689−699

of which are presented in the Supporting Information. Values for $k_{DOM-Cl\bullet}$ ranged from (3.71 ± 0.34) × 10^8 M_C^{-1} s^{-1} (SRNOM I) to (1.52 ± 0.16) × 10^9 M_C^{-1} s^{-1} (SR−TPIN) with an average of (7.99 ± 0.61) × 10^8 M_C^{-1} s^{-1}. The only reported rate constant of DOM with Cl• (1.56 × 10^8 M_C^{-1} s^{-1} for SRNOM I), which was estimated from a modeling analysis of the steady-state concentrations of several radicals in the UV/chlorine treatment,[13] is approximately half of our experimentally determined value of (3.71 ± 0.34) × 10^8 M_C^{-1} s^{-1}. The reaction rate constant determined from complex kinetic modeling suffered from multiple factors (e.g., errors from simplified kinetic equations and optional kinetic parameters) that often differ from the data determined using transient kinetics.[48,49] The rate constants measured by laser flash photolysis or pulse radiolysis are reliable,[49] and allowed us to continue to compare the reaction rates among the 19 DOM samples studied in this work (Table 1). The $k_{DOM-Cl\bullet}$ for fulvic acids (FA) ((6.60 ± 0.63) × 10^8 to (10.38 ± 1.02) × 10^8 M_C^{-1} s^{-1}) were higher than the $k_{DOM-Cl\bullet}$ for humic acids (HA) ((4.26 ± 0.42) × 10^8 to (5.30 ± 0.49) × 10^8 M_C^{-1} s^{-1}) (p < 0.05). Generally, FA exhibits lower M_W and higher hydrophilicity than HA; thus, FA is perhaps more accessible to the Cl• reactions on a per-carbon atom basis.[22] Additionally, $k_{DOM-Cl\bullet}$ of the transphilic DOM isolate was higher than that of the hydrophobic DOM isolate from the same source (e.g., $k_{SL-TPIA-Cl\bullet}$ > $k_{SL-HPOA-Cl\bullet}$ and $k_{WWTP-TPIA-Cl\bullet}$ > $k_{WWTP-HPOA-Cl\bullet}$). The reactivity of EfOM toward Cl• ($k_{EfOM-Cl\bullet}$ = (8.42 ± 0.51) × 10^8 to (13.05 ± 0.89) × 10^8 M_C^{-1} s^{-1}) was relatively high compared to the other DOMs tested. The relatively higher abundance of N- and S-containing functional groups may be partially responsible for the high reactivity of EfOMs.[50,51] Organic nitrogen and sulfur bonds are enriched with electrons and are prone to attack by Cl•.[12,52] Our previous work also concluded that N- and S- containing TrOCs showed quite a high reactivity toward Cl• (e.g. k = (3.12 ± 0.40) × 10^{10} to (4.08 ± 0.24) × 10^{10} M^{-1} s^{-1} for sulfonamides).[8] Despite the differences in the Cl• reaction rate constants with HA, FA, and EfOM, the values of $k_{DOM-Cl\bullet}$ vary within a relatively narrow range ((3.71 ± 0.34) × 10^8 to (1.52 ± 1.56) × 10^9 M_C^{-1} s^{-1}), which is similar to •OH ($k_{DOM-\bullet OH}$ = (1.4 ± 0.2) × 10^8 to (4.5 ± 0.5) × 10^8 M_C^{-1} s^{-1})[9,17] but different from the highly selective radicals (e.g. $SO_4^{\bullet-}$ and $CO_3^{\bullet-}$).[15,16,20,21]

The $k_{DOM-Cl\bullet}$ value represents an averaged value for the Cl• reactions with diverse moieties of DOM and via different reaction channels. Here, we selected seven model compounds to represent different moieties in DOM, including phenol (electron-donating aromatics), benzoic acid and nitrobenzene (electron-withdrawing aromatics), acetic acid and isobutyric acid (aliphatic acids), acetylacetone (ketones), and tyrosine (amino acids). The $k_{DOM-Cl\bullet}$ value was calculated using eq 3:

$$k_{DOM-Cl^\bullet} = \sum \alpha_i k_i \quad (3)$$

where α_i is the carbon proportion of a specific model compound i in the whole DOM molecule, and k_i is the second-order reaction rate constant of model compounds with Cl• expressed in moles carbon. Given the typical DOM aromatic carbon content range of 10−37%,[22] the $k_{DOM-Cl\bullet}$ values calculated using eq 3 are in the range of 1.03−1.23 × 10^9 M_C^{-1} s^{-1} (Table S2). Overall, the model compound experiments showed a relatively small range of $k_{DOM-Cl\bullet}$ values, which is consistent with the relatively narrow range of the experimental $k_{DOM-Cl\bullet}$ values in this study.

Rate Constants between DOM and $Cl_2^{\bullet-}$. The measured rate constants for $Cl_2^{\bullet-}$ with DOMs ranged from (4.60 ± 0.90) × 10^6 M_C^{-1} s^{-1} (SL−HPOA) to (3.57 ± 0.53) × 10^7 M_C^{-1} s^{-1} (LHA) with an average of (1.68 ± 0.25) × 10^7 M_C^{-1} s^{-1} (Table 1). This experimentally determined rate constant range is basically in agreement with Brigante's prediction (10 to 1000 L mgC^{-1} s^{-1} which equates to 1.2 × 10^5 to 1.2 × 10^7 M_C^{-1} s^{-1}).[14,53] When compared against the narrow range of the reaction rates for •OH and Cl• with different sources of DOM (Table 1), the reactivity of $Cl_2^{\bullet-}$ varied with diverse DOMs. The selectivity of $Cl_2^{\bullet-}$ toward different DOM structures may be responsible for the large differences in the $k_{DOM-Cl2\bullet}$ values. $Cl_2^{\bullet-}$ is prone to react with electron-rich moieties (e.g., phenols and anilines), but it is resistant to react with electron-poor moieties (e.g., aliphatic structures and aromatics bearing electron-withdrawing groups).[8,27] For example, the reaction rate constants of $Cl_2^{\bullet-}$ with TrOCs also vary over several orders of magnitudes (<1 × 10^6 to (2.78 ± 0.16) × 10^9 M^{-1} s^{-1}).[8]

In contrast to Cl•, the rate constants of $Cl_2^{\bullet-}$ with FA ((9.90 ± 1.00) × 10^6 to (2.93 ± 0.36) × 10^7 M_C^{-1} s^{-1}) seem to be slightly lower than those with HA ((2.61 ± 0.48) × 10^7 to (3.57 ± 0.53) × 10^7 M_C^{-1} s^{-1}), but there has been no significant statistical derivation (p > 0.05). HA is characterized by higher aromaticity and electron-donating capacity than FA, which may contribute to the slightly higher $k_{DOM-Cl2\bullet-}$ than FA.[22] Among the eight DOM isolates fractionated from water and wastewater in Arizona, $Cl_2^{\bullet-}$ exhibits higher reactivity with EfOM than surface-water DOM (p < 0.05).

Relationships between Reaction Rate Constants and DOM Properties. As the DOM structure becomes more aggregated, the ability of the reactive radical species to "diffuse" with nonplanar DOM structure is restricted. Thus, it could be expected that higher molecular weight DOM have lower reaction rates, which is in fact what was observed. Figure 1 shows that $k_{DOM-Cl\bullet}$ decreased with the increasing M_W values of DOM (R^2 = 0.62). Cl•-induced reactions may be diffusion-controlled in some cases.[8,45,46] The three-dimensional configuration of DOM may become more aggregated with the increase in M_W,[54,55] and the highly compacted inner

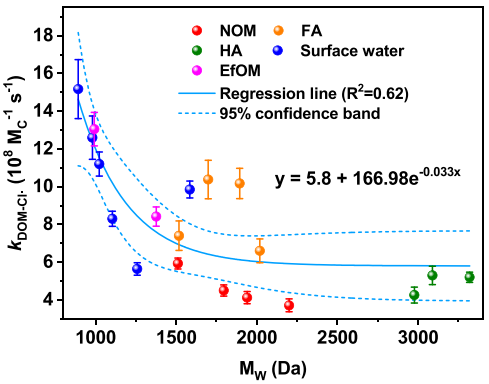

Figure 1. Relationships between weight-averaged molecular weight (M_W) and the second-order reaction rate constants of Cl• with DOM isolates ($k_{DOM-Cl\bullet}$) with the regression line and 95% confidence interval for the regression. Red dots: NOM, orange dots: FA, olive dots: HA, blue dots: surface waters (DOM collected from Salt River and Saguaro Lake in Arizona), magenta dots: EfOM.

https://dx.doi.org/10.1021/acs.est.0c05596
Environ. Sci. Technol. 2021, 55, 689−699

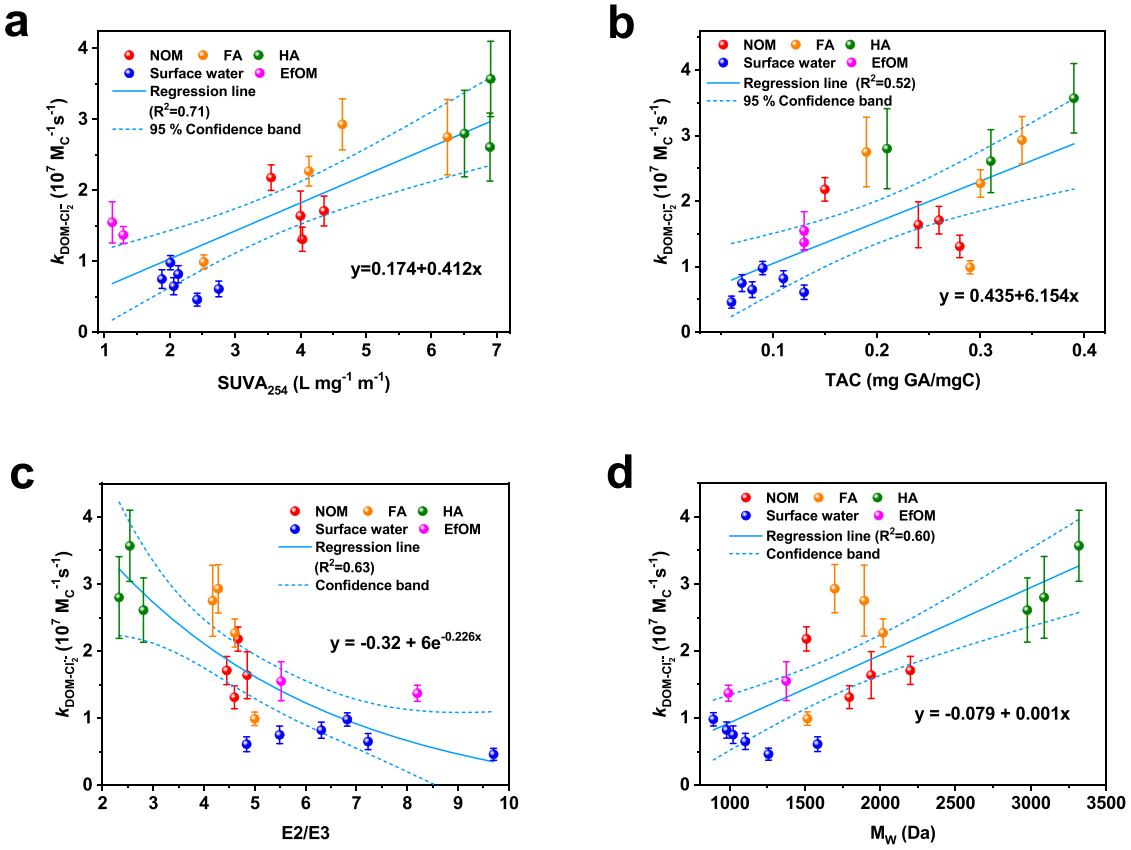

Figure 2. Relationships between $Cl_2^{\bullet-}$ reaction rate constants ($k_{DOM-Cl2\bullet-}$) and different DOM properties (a) SUVA$_{254}$, (b) TAC, (c) E2/E3, and (d) M_W with the regression line and 95% confidence interval for the regression. Red dots: NOM, orange dots: FA, olive dots: HA, blue dots: surface waters (DOM collected from Salt River and Saguaro Lake in Arizona), magenta dots: EfOM.

carbons are not accessibly exposed to Cl$^{\bullet}$; therefore, the apparent $k_{DOM-Cl\bullet}$ on a per-carbon basis may be reduced. To verify this hypothesis, the effect of ionic strength (I) on the $k_{DOM-Cl\bullet}$ values was examined, since the aggregation of DOM was reported to increase with increasing ionic strength.[56] Figure S7 shows that the $k_{DOM-Cl\bullet}$ values for SRNOM II decreased from $(4.12 \pm 0.32) \times 10^8$ to $(2.92 \pm 0.29) \times 10^8$ M_C^{-1} s^{-1}, with the ionic strength increasing from 0 to 1 M. The moderate ionic strength ($I \leq 1$ M) has almost no interference on the kinetics of nonionic reactions (e.g., reactions containing neutral reactants such as Cl$^{\bullet}$);[8,57] therefore, the more aggregation of DOM at higher ionic strength may be responsible for the reduction of $k_{DOM-Cl\bullet}$ values. The inverse associations between the $k_{DOM-\bullet OH}$ values and M_W have also been reported, and they were verified directly by the pulse radiolysis study on molecular weight-fractionated DOM isolates.[9,10,54]

As shown in Figure S8, there was no relationship ($R^2 < 0.3$) between $k_{DOM-Cl\bullet}$ and the other four DOM properties (e.g., SUVA$_{254}$, E2/E3, FI, and TAC). SUVA$_{254}$ is correlated with the aromatic carbon content,[22] and the lack of correlation between the $k_{DOM-Cl\bullet}$ values and SUVA$_{254}$ suggests that nonaromatic moieties in DOMs also react substantially with Cl$^{\bullet}$. This has been shown in the literature where acetate and phenol, which represent aliphatic and aromatic structures present in DOM, have similar carbon-based second-order rate constants with Cl$^{\bullet}$ ($(1.85 \pm 0.20) \times 10^9$ M_C^{-1} s^{-1} for acetate and $(1.87 \pm 0.15) \times 10^9$ M_C^{-1} s^{-1} for phenol; Table S2). Despite exhibiting differing molar-based rate constant values, the rate constant of acetate ($(3.7 \pm 0.4) \times 10^9$ M^{-1} s^{-1}) is lower than that of phenol ($(1.12 \pm 0.09) \times 10^{10}$ M^{-1} s^{-1})).[8,41] Additionally, the lack of a correlation between $k_{DOM-Cl\bullet}$ and the TAC suggests that Cl$^{\bullet}$ would not react selectively with the antioxidant moieties (e.g., phenolic moieties). Specifically, phenol and acetate make equal contributions to the apparent $k_{DOM-Cl\bullet}$ values, but acetate hardly contributes to the TAC. E2/E3, having an inverse relationship with electron-donating components,[15] also had no correlation with $k_{DOM-Cl\bullet}$, indicating that the SET channel from electron-rich moieties was not the only predominant channel in reactions between DOM and Cl$^{\bullet}$. The other reaction channels (i.e., addition and H-abstraction), which are less sensitive to the electronic effects, can also happen in the reaction of Cl$^{\bullet}$ with organics.[8,45,46] In addition, the correlation was also poor between $k_{DOM-Cl\bullet}$ with FI values (a surrogate for microbially or terrestrially derived DOM) (Figure S8).[15]

Different correlations between the DOM properties and reaction rate constants were observed for $Cl_2^{\bullet-}$, and they were compared against those for Cl$^{\bullet}$. Whereas the structure–reactivity relationships with high levels of confidence can be obtained for model compounds,[8] the heterogeneity of DOM often results in less statistically significant relationships. The aromatic carbon content has been widely used as an indicator for DOM reactivity with oxidants.[22,58,59] As shown in Figure 2a, $k_{DOM-Cl2\bullet-}$ appears to be positively correlated with the aromatic carbon contents of DOM (SUVA$_{254}$, R^2 = 0.71). $Cl_2^{\bullet-}$ is highly reactive with aromatics with rate constants in the range of $\sim 10^5$–10^9 M^{-1} s^{-1}, but it is resistant to aliphatic structures with rate constants of only $\sim 10^2$–10^4 M^{-1} s^{-1},[8,27,60] which suggest that the aromatic carbons of DOM predom-

https://dx.doi.org/10.1021/acs.est.0c05596
Environ. Sci. Technol. 2021, 55, 689–699

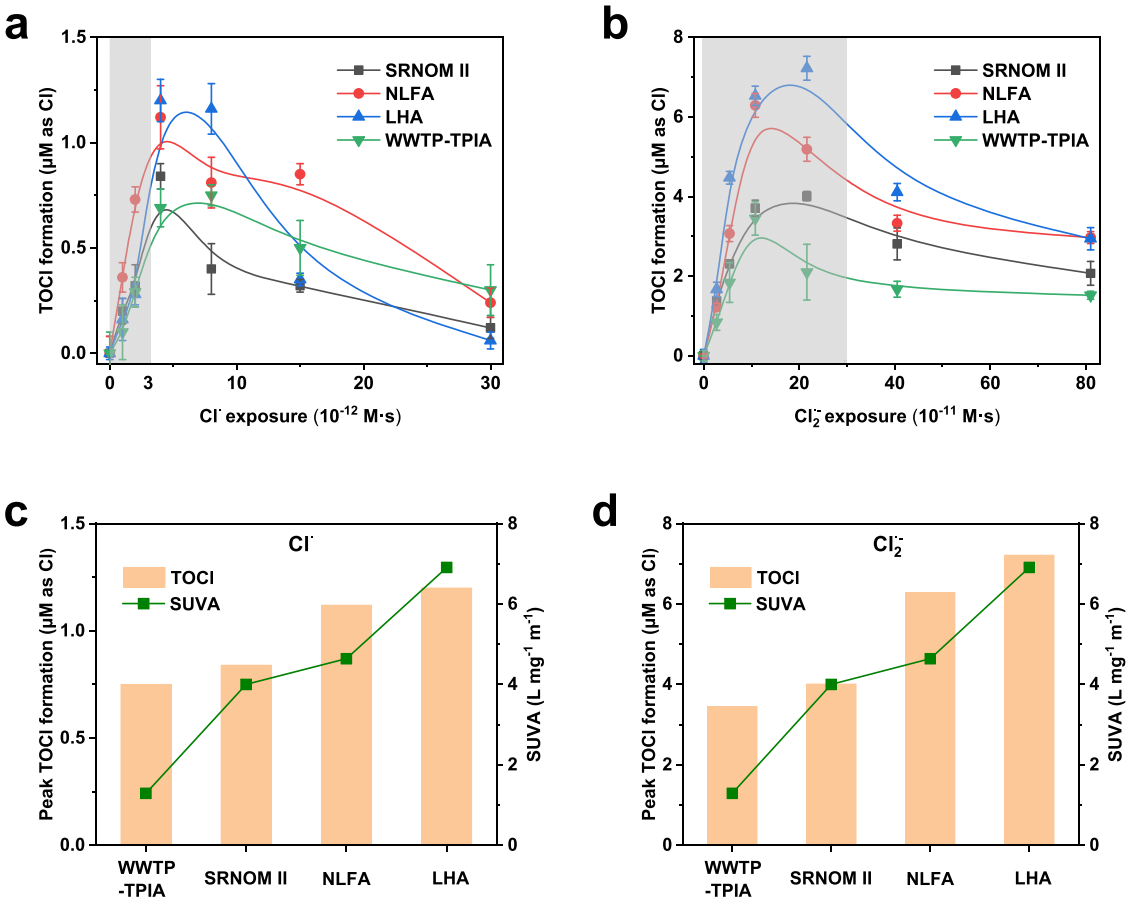

Figure 3. (a, b) Evolution profiles of TOCl concentrations with (a) $Cl^{\bullet}$ oxidant exposure and (b) $Cl_2^{\bullet-}$ oxidant exposure. Conditions: [DOM] = 2.5 $mg_C\ L^{-1}$, pH = 7.0. The gray areas represent typical $Cl^{\bullet}$ exposure (3×10^{-15}–3×10^{-12} M·s) and $Cl_2^{\bullet-}$ exposure (3×10^{-13}–3×10^{-10} M·s) in typical UV-based AOPs. (c, d) Dependence of peak TOCl concentrations formed from DOM reactions with (c) $Cl^{\bullet}$ and (d) $Cl_2^{\bullet-}$ vs SUVA.

inantly contribute the overall reactivity of DOM toward $Cl_2^{\bullet-}$. The $k_{DOM-Cl2\bullet-}$ exhibits a modest positive correlation (R^2 = 0.52) with the TAC values (Figure 2b), indicating that the reactions between $Cl_2^{\bullet-}$ with the antioxidant moieties of DOM such as phenolics are important in contributing to the overall reactions between $Cl_2^{\bullet-}$ and DOM. Figure 2c shows a negative correlation between the $k_{DOM-Cl2\bullet-}$ values and E2/E3 ratios (R^2 = 0.63), indicating $Cl_2^{\bullet-}$ is prone to react with the electron-donating components via the SET channels.[15] $Cl_2^{\bullet-}$ is a selective radical which is prone to attack the electron-rich moieties via the SET mechanism. Although the reaction mechanisms other than SET also exist in reactions between $Cl_2^{\bullet-}$ with organics (e.g., H-abstraction for $Cl_2^{\bullet-}$ with methanol, k = (3.5 ± 0.7) × 10^3 M^{-1} s^{-1}),[27] their rate constants are significantly lower than those of SET reactions (k ~10^7–10^9 M^{-1} s^{-1}), thus resulting in their negligible contribution to the overall $k_{DOM-Cl2\bullet-}$ values. FI shows no relationship with $k_{DOM-Cl2\bullet-}$, indicating that DOM's microbially or terrestrially source is independent of $Cl_2^{\bullet-}$ reactivity with DOM (Figure S8e).

Interestingly, the $k_{DOM-Cl2\bullet-}$ values appeared to be positively related to M_W (R^2 = 0.60, Figure 2d), which was opposite to the relationship of $Cl^{\bullet}$ with M_W (Figure 1). In contrast to $Cl^{\bullet}$, $Cl_2^{\bullet-}$-induced reactions are activation-controlled but not diffusion-controlled. Therefore, the molecular size and the geometry of DOM will not impact the $Cl_2^{\bullet-}$ reactivity from the perspective of diffusion reactions. In fact, higher M_w is found to be associated with higher $SUVA_{254}$ values (R^2 = 0.88, Figure S8f);[22] the apparent relationship between $k_{DOM-Cl2\bullet-}$ and M_W may be artificial, and it represents the relationship between $k_{DOM-Cl2\bullet-}$ and $SUVA_{254}$.

Chlorinated Byproduct Formation from the Reactions of DOM with $Cl^{\bullet}$ and $Cl_2^{\bullet-}$. Four representative DOM isolates with different rate constants with $Cl^{\bullet}$ and $Cl_2^{\bullet-}$, including NOM (SRNOM II), fulvic acid (NLFA), humic acid (LHA), and an EfOM (WWTP−TPIA) were selected to investigate the formation of chlorinated byproducts during their reactions with $Cl^{\bullet}$ or $Cl_2^{\bullet-}$ using laser flash photolysis. The potential generation of HOCl and HOCl-induced TOCl in such a laser system was reasonably ignored due to their extremely low concentrations (the details are presented in Text S7). Figure 3a,b shows the evolution profiles of TOCl yields vs. $Cl^{\bullet}$ or $Cl_2^{\bullet-}$ oxidant exposure (CT value). The background TOCl concentrations, without $Cl^{\bullet}$ or $Cl_2^{\bullet-}$ exposure (i.e., time zero), of the four DOM samples were very low (0.31−0.59 μM) (the details are provided in Table S3) compared against the TOCl levels observed upon exposure to the chlorine radicals. The background TOCl may be from inherent chlorinated compounds in DOM and the potential trace HOCl from $S_2O_8^{2-}$ reacting with Cl^- (although the rate constant between $S_2O_8^{2-}$ and Cl^- is too low to be measured).[61] Therefore, we report the TOCl oxidant exposure yields, which is a result of the subtraction of the background TOCl concentrations from the final TOCl concentrations.

The TOCl yields for the four studied DOMs exhibited increasing followed by decreasing trends with the increases in

https://dx.doi.org/10.1021/acs.est.0c05596
Environ. Sci. Technol. 2021, 55, 689−699

$Cl^{\bullet}$ and $Cl_2^{\bullet-}$ oxidant exposure. For $Cl^{\bullet}$-induced reactions, TOCl reached maximum values at a $Cl^{\bullet}$ exposure range of (4−8) × 10^{-12} M·s (Figure 3a). The maximum TOCl yield was 0.75, 0.84, 1.12, and 1.20 μM for WWTP−TPIA, SRNOM II, NLFA, and LHA, respectively. Overall, the TOCl concentrations became lower with continuous higher $Cl^{\bullet}$ oxidant exposure. For example, the TOCl concentrations decreased by 83% for SRNOM II (from 0.84 to 0.12 μM) and 79% for NLFA (from 1.12 to 0.24 μM) when $Cl^{\bullet}$ exposure increased from 4 × 10^{-12} to 3 × 10^{-11} M·s. For $Cl_2^{\bullet-}$-induced reactions, the maximum TOCl concentrations (e.g., 3.45 μM for WWTP−TPIA to 7.22 μM for LHA) occurred at a $Cl_2^{\bullet-}$ oxidant exposure range of (1.1−2.2) × 10^{-10} M·s (Figure 3b). TOCl formation decreased by nearly half when $Cl_2^{\bullet-}$ exposure nearly quadrupled from 2.2 × 10^{-10} to 8.1 × 10^{-10} M·s. The results clearly confirmed that the interactions between DOM and $Cl^{\bullet}$ or $Cl_2^{\bullet-}$ generate chlorinated byproducts; however, TOCl appears transient. With longer RCS oxidant exposure, continued radical reactions dehalogenate TOCl. This was confirmed by the data shown in Figure S9a,b, where DOM mineralization (i.e., decreasing DOC) was observed with prolonged $Cl^{\bullet}$ or $Cl_2^{\bullet-}$ oxidant exposure. The UVA decrease at extended oxidant exposure (Figure S9c,d) indicated that the attack on aromatic rings by $Cl^{\bullet}$ and $Cl_2^{\bullet-}$ may result in ring opening,[45,46] thereby converting large molecules to small molecules, which is complementary to the DOC reduction. The direct photolysis of chlorinated byproducts during laser irradiation likely contribute little toward the dechlorination of chlorinated byproducts due to the extremely short laser pulse duration (nanosecond levels). However, it cannot be unambiguously neglected because there is also a possibility that some generated organic chlorine has quite high quantum yields and/or molar extinction coefficients. They might still be photolyzed even if the laser duration is extremely short. Potentially, extended oxidant exposure could have increased the polarity of TOCl to such an extent to decrease its affinity for the activated carbon sorbent used in the TOCl analysis;[62,63] thus, the TOCl measured should be considered as a minimum TOCl formed. In the future, additional analytical tools (e.g., LC-QQQ-MS) could be applied to detect lower molecular weight and much more polar TOCl.

Additionally, the peak TOCl yields seemed to be positively dependent on the SUVA values of DOMs for both $Cl^{\bullet}$ and $Cl_2^{\bullet-}$ reactions (Figure 3c,d), suggesting that $Cl^{\bullet}$ − or $Cl_2^{\bullet-}$-induced chlorination mainly occurred at the aromatic moieties of DOM. Notably, $Cl^{\bullet}$ often reacts with aliphatic compounds via H-abstraction, and it can react with aromatics via chlorine addition.[8,41,46,64] In comparison, the reactions of $Cl_2^{\bullet-}$ with the aliphatic moieties of DOM may play a minor role due to low reactivity, and thus the reactions occurring at the aromatic moieties of DOM dominantly contribute to the TOCl formation. In typical UV-based AOPs, the $Cl^{\bullet}$ and $Cl_2^{\bullet-}$ oxidant exposures are estimated to be in the range of 3 × 10^{-15}−3 × 10^{-12} and 3 × 10^{-13}−3 × 10^{-10} M·s, respectively (gray areas in Figure 3a,b, and the details are provided in Text S8). Therefore, during such AOP applications, the $Cl^{\bullet}$ − and $Cl_2^{\bullet-}$-induced TOCl yields should be lower than 1.5 and 8.0 μM, respectively.

Figure S10 shows the formation of TCM during the reactions of DOM with $Cl^{\bullet}$ and $Cl_2^{\bullet-}$. Interestingly, TCM concentrations kept increasing from ND to 1.79 μg L^{-1} (LHA) during the $Cl^{\bullet}$ exposure increase from 0 to 3.0 × 10^{-11} M·s, and they increased from ND to 6.80 μg L^{-1} (SRNOM II) during the $Cl_2^{\bullet-}$ exposure increase from 0 to 8.1 × 10^{-10} M·s. The different trends of TCM (constant increase) from TOCl (increase then decrease) within the studied CT value might be due to the low reactivity of TCM with $Cl^{\bullet}$ and $Cl_2^{\bullet-}$. The second-order rate constant between TCM and $Cl^{\bullet}$ was only 1.2 × 10^7 M^{-1} s^{-1} (in CCl_4), which is significantly lower than those of $Cl^{\bullet}$ with many organics (~10^9 to ~10^{10} M^{-1} s^{-1}, especially 1.8 × 10^{10} M^{-1} s^{-1} for chlorobenzene).[8,41,46,60] The second-order rate constant between TCM and $Cl_2^{\bullet-}$ was not available, but it was expected to be very low because of the low reactivity of aliphatic compounds with $Cl_2^{\bullet-}$.[27] Further oxidation of TCM by $Cl^{\bullet}$ and $Cl_2^{\bullet-}$ is thus difficult.

Formation Mechanisms of Chlorinated Byproducts. The mechanisms of TOCl formation from reactions between DOM and $Cl^{\bullet}$ or $Cl_2^{\bullet-}$ may include the direct addition of $Cl^{\bullet}$ to DOM, the indirect nucleophilic reactions of Cl^- with DOM intermediates (e.g., unprotonated radical DOM(-H)$^{\bullet}$ and cation radical DOM$^{\bullet+}$), and the reactions of $Cl^{\bullet}$ or $Cl_2^{\bullet-}$ with DOM(-H)$^{\bullet}$ and DOM$^{\bullet+}$, as shown in Scheme 1. The first two mechanisms are supported by the findings from the model compound tests in laser flash photolysis experiments (details described in Text S10). The key findings are summarized as follows. First, from the experiments between $Cl^{\bullet}$ and methylparaben (MPB), a phenolic compound present in wastewaters, the signal of MPB−$Cl^{\bullet}$ adducts was observed (Figure 4a). We concluded that the direct addition of $Cl^{\bullet}$ to DOM can generate DOM−$Cl^{\bullet}$ adducts, which could undergo deprotonation and/or react with oxygen, followed by releasing $HO_2^{\bullet}$ to form stable chlorinated products (eq 4).[45,46] No signal of $Cl^{\bullet}$ − adducts (e.g., MPB − $Cl^{\bullet}$ adducts) was observed from the experiments between $Cl_2^{\bullet-}$ and MPB (Figure S11a), indicating that there may be other pathways contributing to the formation of chlorinated byproducts (i.e., the indirect nucleophilic reactions). Second, TMB (1,3,5-trimethoxybenzene) was selected to represent the electron-donating aromatic moieties of DOM. Figure 4b shows that the decay rate constants of TMB$^{\bullet+}$ increased from 2.7 × 10^6 to 5.9 × 10^6 s^{-1} with Cl^- concentration increasing from 0 to 1 M, and the formation of TMB−$Cl^{\bullet}$ adducts was observed. Consequently, we concluded that the nucleophilic reactions between Cl^- and DOM$^{\bullet+}$ could form chlorinated byproducts (eq 5). It should be noted that the phenoxy radical (PhO$^{\bullet}$) would not react with Cl^- to form chlorinated byproducts in environmental-relevant waters (Figure S11d). Third, the potential formation of chlorinated byproducts from the reactions of $Cl^{\bullet}$ or $Cl_2^{\bullet-}$ with DOM(-H)$^{\bullet}$ and DOM$^{\bullet+}$ was

Scheme 1. Proposed Formation Mechanism of Chlorinated Byproducts from DOM Reacting with $Cl^{\bullet}$ or $Cl_2^{\bullet-}$[a]

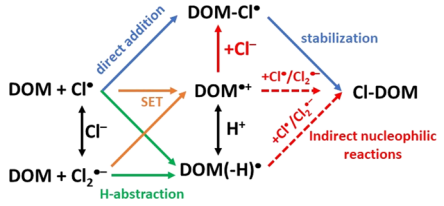

[a]Blue and red arrows represent direct addition and indirect nucleophilic reactions, respectively. SET represents single electron transfer mechanism. Dashed arrows represent speculative pathways from the literature.

https://dx.doi.org/10.1021/acs.est.0c05596
Environ. Sci. Technol. 2021, 55, 689−699

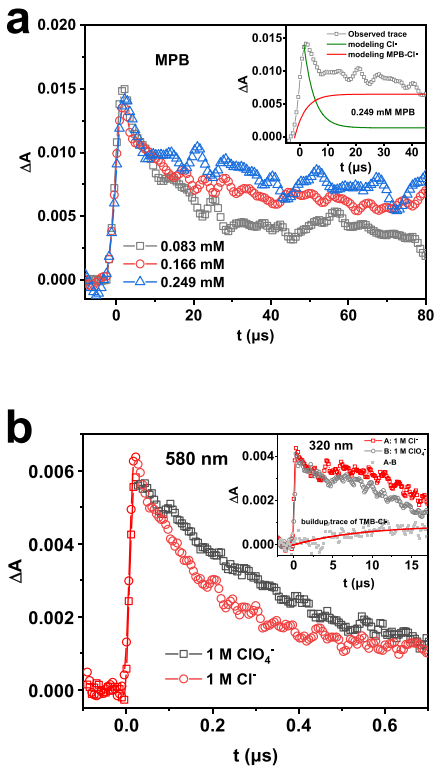

Figure 4. (a) Kinetic traces at 320 nm for methylparaben (MPB) reacting with $Cl^{\bullet}$. Inset: modeling curve of $Cl^{\bullet}$ and the MPB−$Cl^{\bullet}$ adduct. (b) Decay kinetic traces of the 1,3,5-trimethoxybenzene (TMB) cation radical ($TMB^{\bullet+}$) at 1 M Cl^- and 1 M ClO_4^-. Inset: kinetic traces at 320 nm at 1 M Cl^- and 1 M ClO_4^- and the modeling build-up trace of the TMB−$Cl^{\bullet}$ adduct. ClO_4^- was used for ionic strength control.

also proposed based on the extensive literature reports (eqs 6−9).[29,65−69]

$$DOM + Cl^{\bullet} \rightarrow DOM\text{-}Cl^{\bullet}\ adducts \rightarrow Cl\text{-}DOM \quad (4)$$

$$DOM^{\bullet+} + Cl^- \rightarrow DOM\text{-}Cl^{\bullet}\ adducts \rightarrow Cl\text{-}DOM \quad (5)$$

$$DOM(\text{-}H)^{\bullet} + Cl^{\bullet} \rightarrow Cl\text{-}DOM \quad (6)$$

$$DOM^{\bullet+} + Cl^{\bullet} \rightarrow Cl\text{-}DOM + H^+ \quad (7)$$

$$DOM(\text{-}H)^{\bullet} + Cl_2^{\bullet-} \rightarrow Cl\text{-}DOM + Cl^- \quad (8)$$

$$DOM^{\bullet+} + Cl_2^{\bullet-} \rightarrow Cl\text{-}DOM + HCl \quad (9)$$

Environmental Implications. DOM is an important scavenger of $Cl^{\bullet}$ and $Cl_2^{\bullet-}$. The magnitude of the second-order rate constants of DOM from diverse sources with $Cl^{\bullet}$ ($k_{DOM-Cl\bullet}$) and $Cl_2^{\bullet-}$ ($k_{DOM-Cl2\bullet-}$) and the relationships between the kinetic values and DOM properties are important for understanding how not only the DOM concentration but also the nature of DOM influences the extent of chlorine radical scavenging. Kinetic models have been widely used to predict the steady-state levels of radicals and the degradation kinetics of micropollutants in AOPs.[1,2,6,70] The results of this study provide solid data of $Cl^{\bullet}$ and $Cl_2^{\bullet-}$ reaction kinetics with DOM and help to make accurate estimation of the $Cl^{\bullet}$ and $Cl_2^{\bullet-}$ concentrations and associated oxidant exposures.

This study provides direct evidence of the formation of chlorinated byproducts from the reactions of $Cl^{\bullet}$ and $Cl_2^{\bullet-}$ with DOM. Although $Cl^{\bullet}$ and $Cl_2^{\bullet-}$ have been known to be very effective in transforming a variety group of emerging contaminants,[4,6,8] the generation of chlorinated byproducts is inevitable. Reducing the aromaticity of the DOM before the AOP treatment may be helpful in reducing the formation of chlorinated byproducts. This can be accomplished by preoxidation (e.g., ozone),[71] improved coagulation,[72] or adsorption using powder or granular activated carbon.[73] The formation mechanisms include the direct chlorine addition to DOM and the sequential formation from the nucleophilic reactions between the DOM intermediates ($DOM^{\bullet+}$ or $DOM(\text{-}H)^{\bullet}$) and $Cl^{\bullet}$, $Cl_2^{\bullet-}$, or Cl^-. Considering the numerous sources of DOM intermediates in the presence of AOPs and the ubiquitous Cl^- in environmental-relevant waters (e.g., ~10^{-4} M in natural waters),[74,75] the contribution of nucleophilic reactions to the chlorinated byproduct formation may not be negligible and needs further evaluation in future research. Under typical $Cl^{\bullet}$ ($3 \times 10^{-15} - 3 \times 10^{-12}$ M·s) and $Cl_2^{\bullet-}$ exposure ($3 \times 10^{-13} - 3 \times 10^{-10}$ M·s) in AOP processes (e.g., UV/H_2O_2, UV/persulfate, and UV/chlorine), it should be recognized that TOCl is an intermediate. Longer radical oxidant exposure will degrade and partially mineralize TOCl. Optimizing AOP operating conditions should therefore not only consider the effectiveness to oxidize targeted TrOCs but also limit the formation of TOCl molecular structures and their potential associated toxicity induced by the $Cl^{\bullet}$ and $Cl_2^{\bullet-}$ reactions.

■ ASSOCIATED CONTENT

Supporting Information

The Supporting Information is available free of charge at https://pubs.acs.org/doi/10.1021/acs.est.0c05596.

Additional descriptions of chemicals' and DOMs' information, DOM fractionation and characterization methods, laser flash photolysis experiments, $Cl^{\bullet}$ or $Cl_2^{\bullet-}$ reaction rate constants determination, effects of ionic strength on the rate constants, TOCl determination, $Cl^{\bullet}$ or $Cl_2^{\bullet-}$ exposure determination in laser experiments, estimation of $Cl^{\bullet}$ and $Cl_2^{\bullet-}$ exposure in typical AOPs, evolution profile of DOC and SUVA variations, formation of TCM, and time-resolved spectra and kinetic traces for the investigation of TOCl formation mechanism (PDF).

■ AUTHOR INFORMATION

Corresponding Author

Xin Yang − *School of Environmental Science and Engineering, Guangdong Provincial Key Laboratory of Environmental Pollution Control and Remediation Technology, Sun Yat−sen University, Guangzhou 510275, China;* orcid.org/0000-0001-9860-423X; Phone: +86-2039332690; Email: yangx36@mail.sysu.edu.cn

Authors

Yu Lei − *School of Environmental Science and Engineering, Guangdong Provincial Key Laboratory of Environmental Pollution Control and Remediation Technology, Sun Yat−sen University, Guangzhou 510275, China*

Xin Lei − *School of Environmental Science and Engineering, Guangdong Provincial Key Laboratory of Environmental Pollution Control and Remediation Technology, Sun Yat−sen University, Guangzhou 510275, China*

https://dx.doi.org/10.1021/acs.est.0c05596
Environ. Sci. Technol. 2021, 55, 689−699

Paul Westerhoff − *School of Sustainable Engineering and the Built Environment, Arizona State University, Tempe, Arizona 85287−3005, United States;* orcid.org/0000-0002-9241-8759

Xinran Zhang − *School of Environmental Science and Engineering, Guangdong Provincial Key Laboratory of Environmental Pollution Control and Remediation Technology, Sun Yat−sen University, Guangzhou 510275, China*

Complete contact information is available at: https://pubs.acs.org/10.1021/acs.est.0c05596

Notes

The authors declare no competing financial interest.

■ ACKNOWLEDGMENTS

We would like to acknowledge the financial support from the National Key Research and Development Program of China (2017YFE0133200), the National Natural Science Foundation of China (21876210), and the National Science Foundation in the United States of America (EEC-1449500; CBET-1804229).

■ REFERENCES

(1) Lian, L.; Yao, B.; Hou, S.; Fang, J.; Yan, S.; Song, W. Kinetic Study of Hydroxyl and Sulfate Radical-Mediated Oxidation of Pharmaceuticals in Wastewater Effluents. *Environ. Sci. Technol.* **2017**, *51*, 2954−2962.

(2) Cheng, S.; Zhang, X.; Yang, X.; Shang, C.; Song, W.; Fang, J.; Pan, Y. The Multiple Role of Bromide Ion in PPCPs Degradation under UV/Chlorine Treatment. *Environ. Sci. Technol.* **2018**, *52*, 1806−1816.

(3) Liu, Y.; Zhang, J.; Huang, H.; Huang, Z.; Xu, C.; Guo, G.; He, H.; Ma, J. Treatment of Trace Thallium in Contaminated Source Waters by Ferrate Pre-oxidation and Poly Aluminium Chloride Coagulation. *Sep. Purif. Technol.* **2019**, *227*, 115663.

(4) Zhang, K.; Parker, K. M. Halogen Radical Oxidants in Natural and Engineered Aquatic Systems. *Environ. Sci. Technol.* **2018**, *52*, 9579−9594.

(5) Jasper, J. T.; Shafaat, O. S.; Hoffmann, M. R. Electrochemical Transformation of Trace Organic Contaminants in Latrine Wastewater. *Environ. Sci. Technol.* **2016**, *50*, 10198−10208.

(6) Guo, K.; Wu, Z.; Shang, C.; Yao, B.; Hou, S.; Yang, X.; Song, W.; Fang, J. Radical Chemistry and Structural Relationships of PPCP Degradation by UV/Chlorine Treatment in Simulated Drinking Water. *Environ. Sci. Technol.* **2017**, *51*, 10431−10439.

(7) Wardman, P. Reduction Potentials of One-Electron Couples Involving Free Radicals in Aqueous Solution. *J. Phys. Chem. Ref. Data* **1989**, *17*, 513−886.

(8) Lei, Y.; Cheng, S.; Luo, N.; Yang, X.; An, T. Rate Constants and Mechanisms of the Reactions of $Cl^{\bullet}$ and $Cl_2^{\bullet-}$ with Trace Organic Contaminants. *Environ. Sci. Technol.* **2019**, *53*, 11170−11182.

(9) Westerhoff, P.; Mezyk, S. P.; Cooper, W. J.; Minakata, D. Electron Pulse Radiolysis Determination of Hydroxyl Radical Rate Constants with Suwannee River Fulvic Acid and Other Dissolved Organic Matter Isolates. *Environ. Sci. Technol.* **2007**, *41*, 4640−4646.

(10) Rosario-Ortiz, F. L.; Mezyk, S. P.; Doud, D. F. R.; Snyder, S. A. Quantitative Correlation of Absolute Hydroxyl Radical Rate Constants with Non-Isolated Effluent Organic Matter Bulk Properties in Water. *Environ. Sci. Technol.* **2008**, *42*, 5924−5930.

(11) Lei, Y.; Lu, J.; Zhu, M.; Xie, J.; Peng, S.; Zhu, C. Radical Chemistry of Diethyl Phthalate Oxidation via UV/Peroxymonosulfate Process: Roles of Primary and Secondary Radicals. *Chem. Eng. J.* **2020**, *379*, 122339.

(12) Varanasi, L.; Coscarelli, E.; Khaksari, M.; Mazzoleni, L. R.; Minakata, D. Transformations of Dissolved Organic Matter Induced by UV Photolysis, Hydroxyl Radicals, Chlorine Radicals, and Sulfate Radicals in Aqueous-phase UV-Based Advanced Oxidation Processes. *Water Res.* **2018**, *135*, 22−30.

(13) Fang, J.; Fu, Y.; Shang, C. The Roles of Reactive Species in Micropollutant Degradation in the UV/free Chlorine System. *Environ. Sci. Technol.* **2014**, *48*, 1859−1868.

(14) Brigante, M.; Minella, M.; Mailhot, G.; Maurino, V.; Minero, C.; Vione, D. Formation and Reactivity of the Dichloride Radical $Cl_2^{\bullet-}$ in Surface Waters: a Modelling Approach. *Chemosphere* **2014**, *95*, 464−469.

(15) Yan, S.; Liu, Y.; Lian, L.; Li, R.; Ma, J.; Zhou, H.; Song, W. Photochemical Formation of Carbonate Radical and Its Reaction with Dissolved Organic Matters. *Water Res.* **2019**, *161*, 288−296.

(16) Zhou, L.; Sleiman, M.; Ferronato, C.; Chovelon, J.-M.; Richard, C. Reactivity of Sulfate Radicals with Natural Organic Matters. *Environ. Chem. Lett.* **2017**, *15*, 733−737.

(17) Keen, O. S.; McKay, G.; Mezyk, S. P.; Linden, K. G.; Rosario-Ortiz, F. L. Identifying the Factors that Influence the Reactivity of Effluent Organic Matter with Hydroxyl Radicals. *Water Res.* **2014**, *50*, 408−419.

(18) McKay, G.; Dong, M. M.; Kleinman, J. L.; Mezyk, S. P.; Rosario-Ortiz, F. L. Temperature Dependence of the Reaction between the Hydroxyl Radical and Organic Matter. *Environ. Sci. Technol.* **2011**, *45*, 6932−6937.

(19) Lutze, H. V.; Bircher, S.; Rapp, I.; Kerlin, N.; Bakkour, R.; Geisler, M.; Sonntag, C., von; Schmidt, T. C. Degradation of Chlorotriazine Pesticides by Sulfate Radicals and the Influence of Organic Matter. *Environ. Sci. Technol.* **2015**, *49*, 1673−1680.

(20) Canonica, S.; Kohn, T.; Mac, M.; Real, F. J.; Wirz, J.; Gunten, U., von Photosensitizer Method to Determine Rate Constants for the Reaction of Carbonate Radical with Organic Compounds. *Environ. Sci. Technol.* **2005**, *39*, 9182−9188.

(21) Gao, L.; Minakata, D.; Wei, Z.; Spinney, R.; Dionysiou, D. D.; Tang, C.-J.; Chai, L.; Xiao, R. Mechanistic Study on the Role of Soluble Microbial Products in Sulfate Radical-Mediated Degradation of Pharmaceuticals. *Environ. Sci. Technol.* **2019**, *53*, 342−353.

(22) Westerhoff, P.; Aiken, G.; Amy, G.; Debroux, J. Relationships between the Structure of Natural Organic Matter and Its Reactivity towards Molecular Ozone and Hydroxyl Radicals. *Water Res.* **1999**, *33*, 2265−2276.

(23) Chin, Y. P.; Aiken, G.; O'Loughlin, E. Molecular Weight, Polydispersity, and Spectroscopic Properties of Aquatic Humic Substances. *Environ. Sci. Technol.* **1994**, *28*, 1853−1858.

(24) Li, X. F.; Mitch, W. A. Drinking Water Disinfection Byproducts (DBPs) and Human Health Effects: Multidisciplinary Challenges and Opportunities. *Environ. Sci. Technol.* **2018**, *52*, 1681−1689.

(25) Plewa, M. J.; Wagner, E. D.; Metz, D. H.; Kashinkunti, R.; Jamriska, K. J.; Meyer, M. Differential Toxicity of Drinking Water Disinfected with Combinations of Ultraviolet Radiation and Chlorine. *Environ. Sci. Technol.* **2012**, *46*, 7811−7817.

(26) Cuthbertson, A. A.; Kimura, S. Y.; Liberatore, H. K.; Summers, R. S.; Knappe, D. R. U.; Stanford, B. D.; Maness, J. C.; Mulhern, R. E.; Selbes, M.; Richardson, S. D. Does Granular Activated Carbon with Chlorination Produce Safer Drinking Water? From Disinfection Byproducts and Total Organic Halogen to Calculated Toxicity. *Environ. Sci. Technol.* **2019**, *53*, 5987−5999.

(27) Hasegawa, K.; Neta, P. Rate Constants and Mechanisms of Reaction of $Cl_2^{\bullet-}$ Radicals. *J. Phys. Chem.* **1978**, *82*, 854−857.

(28) Bulman, D. M.; Remucal, C. K. Role of Reactive Halogen Species in Disinfection Byproduct Formation during Chlorine Photolysis. *Environ. Sci. Technol.* **2020**, *54*, 9629−9639.

(29) Caregnato, P.; Rosso, J. A.; Soler, J. M.; Arques, A.; Martire, D. O.; Gonzalez, M. C. Chloride Anion Effect on the Advanced Oxidation Processes of Methidathion and Dimethoate: Role of $Cl_2^{\bullet-}$ Radical. *Water Res.* **2013**, *47*, 351−362.

(30) Wang, D.; Bolton, J. R.; Andrews, S. A.; Hofmann, R. Formation of Disinfection By-products in the Ultraviolet/chlorine Advanced Oxidation Process. *Sci. Total Environ.* **2015**, *518-519*, 49−57.

(31) Liu, W.; Cheung, L.-M.; Yang, X.; Shang, C. THM, HAA and CNCl Formation from UV Irradiation and Chlor(am)ination of Selected Organic Waters. *Water Res.* **2006**, *40*, 2033−2043.
(32) Zhao, Q.; Shang, C.; Zhang, X.; Ding, G.; Yang, X. Formation of Halogenated Organic Byproducts during Medium-pressure UV and Chlorine Coexposure of Model Compounds, NOM and Bromide. *Water Res.* **2011**, *45*, 6545−6554.
(33) Yang, X.; Sun, J.; Fu, W.; Shang, C.; Li, Y.; Chen, Y.; Gan, W.; Fang, J. PPCP Degradation by UV/Chlorine Treatment and Its Impact on DBP Formation Potential in Real Waters. *Water Res.* **2016**, *98*, 309−318.
(34) Ike, I. A.; Karanfil, T.; Cho, J.; Hur, J. Oxidation Byproducts from the Degradation of Dissolved Organic Matter by Advanced Oxidation Processes - A Critical Review. *Water Res.* **2019**, *164*, 114929.
(35) Wang, C.; Moore, N.; Bircher, K.; Andrews, S.; Hofmann, R. Full-scale Comparison of UV/H_2O_2 and UV/Cl_2 Advanced Oxidation: The Degradation of Micropollutant Surrogates and the Formation of Disinfection Byproducts. *Water Res.* **2019**, *161*, 448−458.
(36) Baycan, N.; Thomanetz, E.; Sengül, F. Influence of Chloride Concentration on the Formation of AOX in UV Oxidative System. *J. Hazard. Mater.* **2007**, *143*, 171−176.
(37) Leenheer, J. A.; Dotson, A.; Westerhoff, P. Dissolved Organic Nitrogen Fractionation. *Ann. Environ. Sci.* **2007**, *1*, 45−56.
(38) Dotson, A.; Westerhoff, P.; Krasner, S. W. Nitrogen Enriched Dissolved Organic Matter (DOM) Isolates and Their Affinity to Form Emerging Disinfection By-products. *Water Sci. Technol.* **2009**, *60*, 135−143.
(39) Dotson, A. D.; Westerhoff, P.; Ghosh, A., DBP Reactivity of Organic Matter Fractions Collected During Extreme Weather Events. In *Advances in the Physicochemical Characterization of Dissolved Organic Matter: Impact on Natural and Engineered Systems*, American Chemical Society: 2014; *1160*, 257−280, DOI: 10.1021/bk-2014-1160.ch013.
(40) Chen, W.; Westerhoff, P.; Leenheer, J. A.; Booksh, K. Fluorescence Excitation−Emission Matrix Regional Integration to Quantify Spectra for Dissolved Organic Matter. *Environ. Sci. Technol.* **2003**, *37*, 5701−5710.
(41) Buxton, G. V.; Bydder, M.; Salmon, G. A.; Williams, J. E. The Reactivity of Chlorine Atoms in Aqueous Solution Part III. The Reactions of $Cl^•$ with Solutes. *Phys. Chem. Chem. Phys.* **2000**, *2*, 237−245.
(42) Alfassi, Z. B.; Huie, R. E.; Mosseri, S.; Neta, P. Kinetics of One-Electron Oxidation by the ClO Radical. *Int. J. Radiat. Appl. Instrum. Part C. Radiat. Phys. Chem.* **1988**, *32*, 85−88.
(43) Cory, R. M.; Miller, M. P.; McKnight, D. M.; Guerard, J. J.; Miller, P. L. Effect of Instrument-specific Response on the Analysis of Fulvic Acid Fluorescence Spectra. *Limnol. Oceanogr.: Methods* **2010**, *8*, 67−78.
(44) Ainsworth, E. A.; Gillespie, K. M. Estimation of Total Phenolic Content and Other Oxidation Substrates in Plant Tissues using Folin-Ciocalteu Reagent. *Nat. Protoc.* **2007**, *2*, 875−877.
(45) Alegre, M. L.; Gerones, M.; Rosso, J. A.; Bertolotti, S. G.; Braun, A. M.; Martire, D. O.; Gonzalez, M. C. Kinetic Study of the Reactions of Chlorine Atoms and $Cl_2^{•−}$ Radical Anions in Aqueous Solutions. 1. Reaction with Benzene. *J. Phys. Chem. A* **2000**, *104*, 3117−3125.
(46) Mártire, D. O.; Rosso, J. A.; Bertolotti, S.; Roux, G. C. L.; Braun, A. M.; Gonzalez, M. C. Kinetic Study of the Reactions of Chlorine Atoms and $Cl_2^{•−}$ Radical Anions in Aqueous Solutions. II. Toluene, Benzoic Acid, and Chlorobenzene. *J. Phys. Chem. A* **2001**, *105*, 5385−5392.
(47) Hua, Z.; Kong, X.; Hou, S.; Zou, S.; Xu, X.; Huang, H.; Fang, J. DBP Alteration from NOM and Model Compounds after UV/Persulfate Treatment with Post Chlorination. *Water Res.* **2019**, *158*, 237−245.
(48) Wojnárovits, L.; Tóth, T.; Takács, E. Critical Evaluation of Rate Coefficients for Hydroxyl Radical Reactions with Antibiotics: A Review. *Crit. Rev. Environ. Sci. Technol.* **2018**, *48*, 575−613.
(49) Wojnárovits, L.; Takács, E. Rate Constants of Sulfate Radical Anion Reactions with Organic Molecules: A Review. *Chemosphere* **2019**, *220*, 1014−1032.
(50) Niu, X.-Z.; Harir, M.; Schmitt-Kopplin, P.; Croué, J.-P. Characterisation of Dissolved Organic Matter using Fourier-Transform Ion Cyclotron Resonance Mass Spectrometry: Type-Specific Unique Signatures and Implications for Reactivity. *Sci. Total Environ.* **2018**, *644*, 68−76.
(51) Gonsior, M.; Zwartjes, M.; Cooper, W. J.; Song, W.; Ishida, K. P.; Tseng, L. Y.; Jeung, M. K.; Rosso, D.; Hertkorn, N.; Schmitt-Kopplin, P. Molecular Characterization of Effluent Organic Matter Identified by Ultrahigh Resolution Mass Spectrometry. *Water Res.* **2011**, *45*, 2943−2953.
(52) Wang, Y.; Couet, M.; Gutierrez, L.; Allard, S.; Croué, J. P. Impact of DOM Source and Character on the Degradation of Primidone by UV/Chlorine: Reaction Kinetics and Disinfection By-product Formation. *Water Res.* **2020**, *172*, 115463.
(53) Neta, P.; Huie, R. E.; Ross, A. B. Rate Constants for Reactions of Inorganic Radicals in Aqueous Solution. *J. Phys. Chem. Ref. Data* **1988**, *17*, 1027−1284.
(54) Dong, M. M.; Mezyk, S. P.; Rosario-Ortiz, F. L. Reactivity of Effluent Organic Matter (EfOM) with Hydroxyl Radical as a Function of Molecular Weight. *Environ. Sci. Technol.* **2010**, *44*, 5714−5720.
(55) Tsaih, M. L.; Chen, R. H. Effect of Molecular Weight and Urea on the Conformation of Chitosan Molecules in Dilute Solutions. *Int. J. Biol. Macromol.* **1997**, *20*, 233−240.
(56) Pan, B.; Ghosh, S.; Xing, B. Dissolved Organic Matter Conformation and Its Interaction with Pyrene As Affected by Water Chemistry and Concentration. *Environ. Sci. Technol.* **2008**, *42*, 1594−1599.
(57) Jacobi, H. W.; Wicktor, F.; Herrmann, H.; Zellner, R. Laser Flash Photolysis Kinetic Study of Reactions of the $Cl_2^{•−}$ Radical Anion with Oxygenated Hydrocarbons in Aqueous Solution. *Int. J. Chem. Kinet.* **1999**, *31*, 169−181.
(58) Reckhow, D. A.; Singer, P. C.; Malcolm, R. L. Chlorination of Humic Materials: Byproduct Formation and Chemical Interpretations. *Environ. Sci. Technol.* **1990**, *24*, 1655−1664.
(59) Westerhoff, P.; Chao, P.; Mash, H. Reactivity of Natural Organic Matter with Aqueous Chlorine and Bromine. *Water Res.* **2004**, *38*, 1502−1513.
(60) National Institute of Standards and Technology. *NDRL/NIST Solution Kinetics Database on the Web*. http://kinetics.nist.gov/ (accessed May 20, 2020).
(61) Lee, J.; von Gunten, U.; Kim, J. H. Persulfate-Based Advanced Oxidation: Critical Assessment of Opportunities and Roadblocks. *Environ. Sci. Technol.* **2020**, *54*, 3064−3081.
(62) Kinani, A.; Salhi, H.; Bouchonnet, S.; Kinani, S. Determination of Adsorbable Organic Halogens in Surface Water Samples by Combustion−Microcoulometry versus Combustion−Ion Chromatography Titration. *J. Chromatogr. A* **2018**, *1539*, 41−52.
(63) Chen, B.; Bu, Y.; Yang, J.; Nian, W.; Hao, S. Methods for Total Organic Halogen (TOX) Analysis in Water: Past, Present, and Future. *Chem. Eng. J.* **2020**, *399*, 125675.
(64) Minakata, D.; Kamath, D.; Maetzold, S. Mechanistic Insight into the Reactivity of Chlorine-Derived Radicals in the Aqueous-Phase UV−Chlorine Advanced Oxidation Process: Quantum Mechanical Calculations. *Environ. Sci. Technol.* **2017**, *51*, 6918−6926.
(65) Vione, D.; Maurino, V.; Minero, C.; Calza, P.; Pelizzetti, E. Phenol Chlorination and Photochlorination in the Presence of Chloride Ions in Homogeneous Aqueous Solution. *Environ. Sci. Technol.* **2005**, *39*, 5066−5075.
(66) Anipsitakis, G. P.; Dionysiou, D. D.; Gonzalez, M. A. Cobalt-Mediated Activation of Peroxymonosulfate and Sulfate Radical Attack on Phenolic Compounds. Implications of Chloride Ions. *Environ. Sci. Technol.* **2006**, *40*, 1000−1007.

(67) Cai, W.-W.; Peng, T.; Yang, B.; Xu, C.; Liu, Y.-S.; Zhao, J.-L.; Gu, F.-L.; Ying, G.-G. Kinetics and Mechanism of Reactive Radical Mediated Fluconazole Degradation by the UV/chlorine Process: Experimental and Theoretical Studies. *Chem. Eng. J.* **2020**, *402*, 126224.
(68) Cook, C. D.; Woodworth, R. C. Oxidation of Hindered Phenols. II. The 2,4,6-Tri-t-butylphenoxy Radical. *J. Am. Chem. Soc.* **1953**, *75*, 6242−6244.
(69) Altwicker, E. R. The Chemistry of Stable Phenoxy Radicals. *Chem. Rev.* **1967**, *67*, 475−531.
(70) Bulman, D. M.; Mezyk, S. P.; Remucal, C. K. The Impact of pH and Irradiation Wavelength on the Production of Reactive Oxidants during Chlorine Photolysis. *Environ. Sci. Technol.* **2019**, *53*, 4450−4459.
(71) Wenk, J.; Aeschbacher, M.; Salhi, E.; Canonica, S.; von Gunten, U.; Sander, M. Chemical Oxidation of Dissolved Organic Matter by Chlorine Dioxide, Chlorine, and Ozone: Effects on its Optical and Antioxidant Properties. *Environ. Sci. Technol.* **2013**, *47*, 11147−11156.
(72) Lin, J.-L.; Ika, A. R. Minimization of Halogenated DBP Precursors by Enhanced PACl Coagulation: The Impact of Organic Molecule Fraction Changes on DBP Precursors Destabilization with Al Hydrates. *Sci. Total Environ.* **2020**, *703*, 134936.
(73) Zusman, O. B.; Kummel, M. L.; De la Rosa, J. M.; Mishael, Y. G. Dissolved Organic Matter Adsorption from Surface Waters by Granular Composites versus Granular Activated Carbon Columns: An Applicable Approach. *Water Res.* **2020**, *181*, 115920.
(74) Vione, D.; Carena, L. The Possible Production of Harmful Intermediates Is the ″Dark Side″ Of the Environmental Photochemistry of Contaminants (Potentially Adverse Effects, And Many Knowledge Gaps). *Environ. Sci. Technol.* **2020**, *54*, 5328−5330.
(75) Vione, D.; Falletti, G.; Maurino, V.; Minero, C.; Pelizzetti, E.; Malandrino, M.; Ajassa, R.; Olariu, R.-I.; Arsene, C. Sources and Sinks of Hydroxyl Radicals upon Irradiation of Natural Water Samples. *Environ. Sci. Technol.* **2006**, *40*, 3775−3781.

https://dx.doi.org/10.1021/acs.est.0c05596
Environ. Sci. Technol. 2021, 55, 689−699